

Estimating the value of containment strategies in delaying the arrival time of an influenza pandemic: A case study of travel restriction and patient isolation

Lin Wang, Yan Zhang, Tianyi Huang, and Xiang Li*
*Adaptive Networks and Control Laboratory, Department of Electronic
Engineering, Fudan University, Shanghai 200433, P.R.China*

With a simple phenomenological metapopulation model, which characterizes the invasion process of an influenza pandemic from a source to a subpopulation at risk, we compare the efficiency of inter- and intra-population interventions in delaying the arrival of an influenza pandemic. We take travel restriction and patient isolation as examples, since in reality they are typical control measures implemented at the inter- and intra-population levels, respectively. We find that the intra-population interventions, e.g., patient isolation, perform better than the inter-population strategies such as travel restriction if the response time is small. However, intra-population strategies are sensitive to the increase of the response time, which might be inevitable due to socioeconomic reasons in practice and will largely discount the efficiency.

PACS numbers: 87.23.Kg,87.10.Ed,87.19.X-

I. INTRODUCTION

During the past decades, extensive efforts have been made to investigate the spread of epidemics. Besides various epidemiological models having been proposed to explore virus transmission in a closed population[1], the study of network spreading uses structured populations to understand the evolution of epidemics in more realistic social settings[2–5]. These studies have contributed a great deal of insightful findings, such as the absence of epidemic threshold in scale-free networks[6], the reaction-diffusion process, and metapopulation[7, 8], to name a few. These significant advances have raised new issues on how to limit or control the spread of infectious diseases in human society.

To curb the spatial spread of diseases from city to city, a variety of strategies are recommended according to World Health Organization(WHO) or United States(US) response plans[9]: (i) Vaccination of prior groups or dynamic mass vaccination; (ii) antiviral drugs for prophylaxis and treatment; (iii) community-based prevention and control; and (iv) travel-related containment measures. Except for the fact that travel-related measures are implemented at the inter-city level, other strategies are mainly performed at the intra-city level. The first two pharmaceutical interventions cut down the number of potential susceptibles or allay the virus transmission rate, respectively. Community-based strategies might affect individuals (e.g., patient isolation, self-isolation, quarantine), groups, or entire communities (e.g., cancellation of public gatherings, school closures) in a city. Travel-related measures mainly result in the restriction or cancellation of nonessential trips.

By supposing that the outbreak of a pandemic is underway, many works have studied the efficiency of strategies by using the metapopulation model, which harnesses

the reaction-diffusion framework to sketch human daily contacts and mobility. The epidemic reaction takes place inside each subpopulation due to personal contacts, and the infectious disease cascades subpopulation by subpopulation via the travel of individuals (here each city is represented by a subpopulation). The importance of various strategies in decreasing the attack rate or prevalence has been extensively studied in Refs. [10, 11] mainly by computational simulations. Particularly, by analyzing the delay of arrival time of the disease [12–16], it has been shown that the efficiency of travel restriction in slowing down the international spread of pandemic influenza is limited.

In these seminal works, the intra- and inter-population interventions are seldom compared with each other to provide a holistic picture about their value in delaying disease invasion. This should give us pause for thought. Whether it is reasonable to discard the tactic of travel restriction might also depend on how good the intra-population strategies perform. In an attempt to study this issue, we theoretically analyze the efficiency of two kinds of typical containment strategies, namely, travel restriction and patient isolation, which are implemented at the inter- and intra-population levels, respectively. We mainly use a simple phenomenological model following Refs. [16, 17], which considers the importation of an infectious disease from a source to a region at risk during the early stage of a pandemic outbreak. Since the spreading process cascades subpopulation by subpopulation, this two-subpopulation version[15] is a simple model but rational approximation of the initial stage of the pandemic. We mainly focus on the impact of strategies to delay the arrival time of disease in the subpopulation at risk, because no outbreak will occur in an unaffected region before the introduction of infectious seeds. After the disease lands in the subpopulation, the ongoing endogenous transmission will become the mainstream of infections[11, 15]. Thus the first arrival time of infectious travelers is an important quantity characterizing the timing of the disease outbreak[16, 18, 19].

*lix@fudan.edu.cn

II. MODEL DESCRIPTION

To build the model, we first specify the mechanism of individual mobility between subpopulations x, y . Following Refs. [16–19], at every time step, each individual may travel from his current location $x(y)$ to a neighboring subpopulation $y(x)$ with a per capita diffusion rate $\omega_{xy}(\omega_{yx})$. We define the unit time as 1 day. The model proceeds with discrete time steps. In reality, the amount of transportation flows, e.g., air traffic, between cities is often symmetric[18–20], which indicates a detailed balance for the traffic flows. For simplicity, we assume that the subpopulations x, y have the same population size $N_x = N_y = N$ and diffusion rate $\omega_{xy} = \omega_{yx} = \omega$. Thus there are on average ωN individuals departing from each subpopulation per day. Note that relaxing these two restrictions does not change the main results of this Brief Report as long as we maintain a detailed balance condition. While mobility couples different locations, the epidemic reaction process occurs in each subpopulation, where the population is mixing homogeneously. We consider a standard susceptible-infective-removed (SIR) compartment model to represent the influenza-like illness[7, 8, 10]. At a given time t , the number of susceptible, infectious, and recovered individuals in $x(y)$ are defined as $S_x(t), I_x(t), R_x(t)(S_y(t), I_y(t), R_y(t))$, respectively. The SIR reaction is governed by the transition rates μ and β [1]. In a unit time, an infectious one recovers and becomes immune at the rate μ . The parameter β characterizes disease transmissibility, which reflects the combined factors of the virus transmission rate and individual contact rate per unit time[8]. A susceptible individual might acquire infection by contact with infectious ones staying in the same subpopulation. With the mean-field approximation, at time t , the probability for a susceptible one in subpopulation $x(y)$ to acquire infection is found by multiplying the density of infectious $I_x(t)/N(I_y(t)/N)$ by β [1]. In this baseline case, the transfer of susceptible and infectious individuals is ruled by the diffusion rate ω . The epidemic threshold is determined by the basic reproductive number $R_0 = \beta/\mu$, which identifies the expected number of secondary infections produced by an infected individual during his infectious period in an entire susceptible population[1].

We next specify the dynamics under interventions. Since many socioeconomic factors might defer the implementation of strategies, we define a response time t_0 representing the time interval between the actual inception of an outbreak and the time when the strategies become available. Travel restriction (TR) mainly affects individual mobility between two subpopulations. We define the parameter α as the intensity of TR, which means that a reduction of fraction α in travel begins at time t_0 , i.e., in the model, we decrease the diffusion rate from ω to $(1 - \alpha)\omega$ after time t_0 .

Patient isolation (PI) mainly impacts individual compartment transitions. The effect of PI may relate to enforcement by local authorities, or is attributed to the self-

isolation of infected individuals. For simplicity, we do not distinguish between these two aspects. The parameter η is defined to reflect the intensity of PI. It means that on average a fraction η of infectious persons will be isolated per unit time after t_0 . We introduce the PI by adding an isolation process that each infectious one has a likelihood to be isolated with rate η per unit time. Since these isolating individuals have little chance to cause infection, we remove them as long as they are isolated.

III. ANALYTICAL AND SIMULATION RESULTS

Initially, an infectious individual is introduced into subpopulation x . Thus the initial condition is $I_x(0)=1, I_y(0)=0$. We first analyze the efficiency of TR in slowing down disease invasion to subpopulation y . The key issue is to evaluate its impact on delaying the first arrival time(FAT) of infectious travelers from x . With the Poisson process assumption that the diffusion of any individual is independent from that of others, the probability that the first infectious individual arrives in subpopulation y at time $t^y = t$ is

$$P(t^y = t) = [1 - (1 - \omega)^{I_x(t)}] \prod_{t_i=1}^{t-1} (1 - \omega)^{I_x(t_i)}, \quad (1)$$

which describes that at least one successful transfer of infectious individuals from subpopulation x to y occurs at time t , and none at previous time steps[18, 19]. In reality, it is general that the number of travelers per day is several orders of magnitude smaller than the total population of a city, where only small amounts of people leave to travel per day. Empirical evidence of worldwide or US domestic air transportation[7] suggests that the daily diffusion rate of individuals on each flight route is of the order 10^{-4} or less. We here assume $\omega = 10^{-4}, N = 10^6$. Using the Taylor expansion, Eq. (1) becomes $P(t^y = t) = \omega I_x(t) \exp[-\omega \sum_{0 < t_i < t} I_x(t_i)]$.

Based on many seminal works[10–16], we assume a pandemic influenza with $R_0 = 1.75$ and the infectious period $\mu^{-1} = 3$ days. In this case, the Malthusian parameter λ , the real-time exponential growth rate at the early stage of an outbreak[21, 22], is $\beta - \mu = 0.25$. Since $\omega \ll \lambda$, the SIR reaction happens at a time scale much faster than the diffusion process, thus the number of infectious individuals in subpopulation x grows sufficiently before subpopulation y is invaded. Meanwhile, at this early stage, the infectious ones only make up a small fraction of the total population in $x, I_x(t) \ll N$. With a mean-field approximation for the evolution of infectious individuals, we have[3, 18, 19] $I_x(t_i) \simeq I_x(0) \exp(\lambda t_i)$, $t_i \leq t^y$. Using the continuum approximation $\sum_{0 < t_i < t} I_x(t_i) = \int_0^t d\tau I_x(\tau)$, we obtain the probability density of FAT, $P^F(t) = \omega \exp[\lambda t - (\omega/\lambda) \exp(\lambda t)]$, with the mean value $\langle t^F \rangle = (1/\lambda)(\ln(\lambda/\omega) - \gamma)$ [18, 19], where γ is the Euler constant. With the above given parameters, this characteristic time scale of FAT is $\langle t^F \rangle \simeq 29$ days.

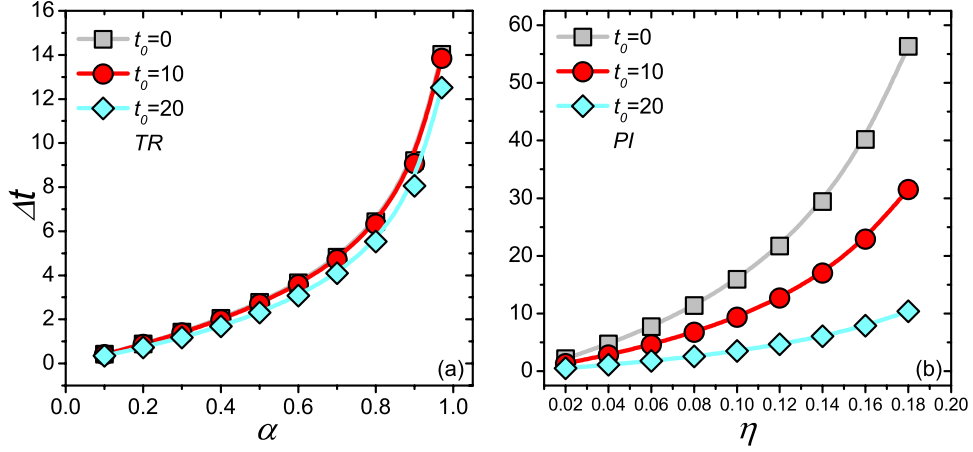


FIG. 1: (*Color online*) The analytical results of the relation between the delay of FAT, Δt , and the intensity of strategies. (a) Travel restriction. (b) Patient isolation. The colored squares, circles, and diamonds refer to the cases of $t_0=0$, 10, and 20 days, respectively.

In the TR scenario, when the FAT is smaller than the response time t_0 , the probability density of FAT is still $P(t)$; however, when the FAT is larger than t_0 , this probability density becomes $P_\alpha(t) = (1 - (1 - \alpha)\omega)^{I_x(t)} \prod_{0 < t_i < t_0} (1 - \omega)^{I_x(t_i)} \prod_{t_0 \leq t_j < t} (1 - (1 - \alpha)\omega)^{I_x(t_j)} \simeq (1 - \alpha)\omega \exp[\lambda t - (1 - \alpha)\omega \exp(\lambda t)/\lambda - \alpha\omega \exp(\lambda t_0)/\lambda]$. We numerically calculate the average FAT through $\langle t_\alpha^F \rangle = \int_0^{t_0} \tau P(\tau) d\tau + \int_{t_0}^\infty \tau P_\alpha(\tau) d\tau$, and get the delay of FAT, $\Delta t(\alpha)$, by solving

$$\Delta t(\alpha) = \langle t_\alpha^F \rangle - \langle t^F \rangle. \quad (2)$$

If the response time t_0 is negligible ($t_0 = 0$), Eq.(2) is simplified as

$$\Delta t(\alpha)|_{t_0=0} = -\ln(1 - \alpha)/\lambda, \quad (3)$$

which recovers the results obtained by the cumulative probability $P(t^y \leq t)$ in Refs. [15, 16]. Note that Eq (3) is independent from the values of ω, N . With $\lambda=0.25$, unless the intensity α is increased to an unpractically high level ($\alpha > 0.97$), $\Delta t(\alpha)$ cannot be longer than 2 weeks.

To study the PI scenario, we first consider the case where the FAT is larger than t_0 . At this early stage, we still have the approximation $I_x(t_i) \simeq \exp(\lambda t_i)$ when time $t_i \leq t_0$; after t_0 , the Malthusian parameter becomes $\lambda_\eta = \lambda - \eta$, and thus we have $I'_x(t_j) \simeq \exp(\eta t_0) \exp(\lambda_\eta t_j)$ when $t_0 < t_j \leq t^y$. The probability density in this case is $P_\eta(t) = (1 - (1 - \omega)^{I'_x(t)}) \prod_{0 < t_i \leq t_0} (1 - \omega)^{I_x(t_i)} \prod_{t_0 < t_j < t} (1 - \omega)^{I'_x(t_j)} \simeq \omega I'_x(t) \exp(-\omega \int_0^{t_0} I_x(\tau) d\tau) \exp(-\omega \int_{t_0}^t I'_x(\tau) d\tau) = \omega \exp[\Theta(t_0)] \exp[\lambda_\eta t - \omega \exp(\eta t_0 + \lambda_\eta t)/\lambda_\eta]$, where $\Theta(t_0) = \eta t_0 - \omega \exp(\lambda t_0)/\lambda + \omega \exp(\lambda t_0)/\lambda_\eta$. If the response time is negligible ($t_0=0$), we simplify the former expression as $P_\eta(t)|_{t_0=0} \simeq \omega \exp[\lambda_\eta t - \omega \exp(\lambda_\eta t)/\lambda_\eta]$, which leads to the average FAT, $\langle t_\eta^F \rangle|_{t_0=0} = \int_0^\infty \tau P_\eta(\tau)|_{t_0=0} d\tau \simeq (\ln(\lambda_\eta/\omega) - \gamma)/\lambda_\eta$. In this case,

we get the relation between Δt and η by solving the equation

$$\Delta t(\eta)|_{t_0=0} = \langle t_\eta^F \rangle|_{t_0=0} - \langle t^F \rangle \quad (4)$$

If $t_0 > 0$, the average FAT is numerically integrated via the equation $\langle t_\eta^F \rangle = \int_0^{t_0} \tau P(\tau) d\tau + \int_{t_0}^\infty \tau P_\eta(\tau) d\tau$. We therefore have the relation between Δt and η as

$$\Delta t(\eta) = \langle t_\eta^F \rangle - \langle t^F \rangle. \quad (5)$$

With Eq. (4) and $\lambda = 0.25$, we find that an intermediate level of the strategy intensity $\eta = 0.12$ can adequately suspend the arrival of disease to subpopulation y for more than 3 weeks. When the response time $t_0 = 0$, we conclude that the strategy of PI performs better than the TR. This is mainly because the TR alone can not mitigate the initial exponential growth of infectious ones in the source. However, the strategy of PI is highly sensitive to the increase of the response time t_0 . As shown in Fig. 1, when t_0 increases from 0 to 20 days, there is an evident decline for the delay $\Delta t(\eta)$ in the PI scenario, while the delay $\Delta t(\alpha)$ actualized by implementing the TR is robust to the increase of t_0 .

We further use the dynamic Monte Carlo method to simulate the epidemic evolution under different interventions. The simulations are performed with discrete time steps, and we update each individual's behavior in parallel per unit time. The parameters are $N = 10^6$, $\omega = 10^{-4}$, $R_0 = 1.75$, and $\mu^{-1} = 3$ days. Initially, an infectious individual is introduced into subpopulation x , and thus the initial condition is $I_x(0)=1, I_y(0)=0$. When the containment strategies are excluded, the epidemic reaction and diffusion at each unit time proceed as follows. (i) Reaction: Inside each subpopulation, individuals are mixing homogeneously. At time t , the probability for any susceptible in subpopulation $x(y)$ to acquire infection is $\beta I_x(t)/N(\beta I_y(t)/N)$. The number of new infections in $x(y)$ at time t is extracted from a binomial distribution

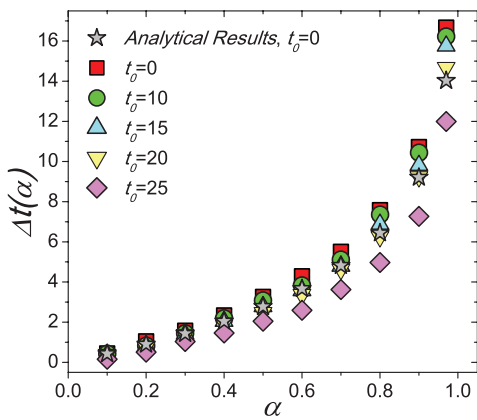


FIG. 2: (*Color online*) The relation between the delay of FAT, $\Delta t(\alpha)$, and the intensity of travel restriction. The gray stars are the analytical results with $t_0 = 0$. The other colored symbols are the simulation results with various response times $t_0=0, 10, 15, 20$, and 25 days.

with probability $\beta I_x(t)/N(\beta I_y(t)/N)$ and the number of trials $S_x(t)(S_y(t))$. The number of recovered individuals in $x(y)$ is also extracted from a binomial distribution with probability μ and the number of trials $I_x(t)(I_y(t))$. (ii) Diffusion: After all individuals have been updated for the reaction, we simulate their diffusion. The number of susceptible travelers departing from each subpopulation per unit time is also extracted from a binomial distribution with probability ω and the number of trials $S_x(t)(S_y(t))$. The number of infectious and recovered travelers is obtained in the same way.

We first study the effects of TR in delaying the arrival of disease to subpopulation y . To assemble this factor into the simulation, we rescale the per capita diffusion rate ω by a multiplier $1 - \alpha$, where the parameter α reflects the intensity of TR. The strategy is activated after a given response time t_0 . Figure 2 provides a holistic view about the relation between the delay of FAT, $\Delta t(\alpha)$, and the restriction intensity α . Since the disease might die out due to randomness, every data point is obtained by averaging the simulations with the successful transfer of infectious ones among 10^4 times of Monte Carlo random experiments, each of which is simulated with 500 time steps. The gray stars are the analytical results obtained by Eq. (3), which agree well with the simulations. When $\alpha = 0.3, 0.6$, and 0.9 and $t_0 = 0$, the simulations show that $\Delta t(\alpha) \simeq 2, 4$, and 11 days, respectively. Even if the restriction intensity is elevated to an unpractically high level, e.g., $\alpha = 0.97$, $\Delta t(\alpha)$ is still less than 3 weeks. It is clear that Δt is small if the time scale of the initial exponential growth $1/\lambda$ is small [see Eq. 3]. We further study the impact of the response time on the efficiency of TR. In Fig. 2, unless t_0 approaches $\langle t^F \rangle$, which is the average FAT without TR, and α is large, there is no evident decline for the simulation results of $\Delta t(\alpha)$.

We next study the effects of PI in delaying disease invasion. To introduce this factor in the model, we add

an isolation process before the reaction process at each time step after t_0 . The parameter η reflects the intensity of PI. Per unit time, the number of newly isolated individuals in subpopulation $x(y)$ is extracted from a binomial distribution with probability η and the number of trials $I_x(t)(I_y(t))$. Figure 3(a) presents the relation between the delay of FAT, Δt , and the isolation intensity η with $t_0 = 0$. For each η , we perform 10^4 times of Monte Carlo random experiments, each of which is simulated with 500 time steps. Due to the randomness embedded in the dynamical process, the infectious individuals in source x might be totally eradicated before traveling to subpopulation y . With a given η , we measure $\Delta t(\eta)$ by averaging the simulations that the infectious ones from source x successfully jump to subpopulation y . The results are highlighted by the red squares in Fig. 3(a). The gray stars are the analytical results obtained by Eq.(4). If the isolation intensity η is at a small or intermediate level ($\eta \leq 0.18$), the simulation results agree well with the theoretical predications. However, if the intensity η is extremely large, the simulations obviously deviate from the analytical results. In this latter case, since the Malthusian parameter λ_η is quite small, there is a huge likelihood of totally eradicating the infectious individuals at the early stage of an outbreak due to randomness. For instance, when $\eta = 0.2, 0.22$, the fraction of eradication in all independent modeling realizations reaches 97.7% and 99.2%, respectively, while for $\eta = 0.12$, the fraction of eradication is only 75.6% [see the dark cyan diamonds in Fig.3(a)]. If $\eta \geq 0.25$, the Malthusian parameter $\lambda \leq 0$, the disease hardly persists in the population. With the same condition that $t_0 = 0$, the strategy of PI is more efficient than TR: An intermediate level of isolation intensity η can adequately delay the arrival of disease for about 1 month.

Figure 3(b) shows the impact of the response time t_0 on the delaying effects of PI. For a small t_0 , e.g., $t_0 = 10$, which is much smaller than $\langle t^F \rangle$, an intermediate level of PI (e.g., $\eta = 0.14$) still suspends the arrival of disease for about 3 weeks. This achievement exceeds the performance of TR even with an extremely high restriction intensity. The simulations also illuminate that the PI is sensitive to the increase of t_0 . There is a remarkable decline in the simulation results of $\Delta t(\eta)$ when t_0 approaches $\langle t^F \rangle$. For instance, 25 days of waiting to implement the strategy ($t_0 = 25$) will only postpone the arrival of disease in subpopulation y for about 2 weeks at most.

Actually, other intra-population interventions can also be analyzed under this framework. For instance, social distancing limits public activities to reduce personal contacts, which can be reflected by rescaling the disease transmission rate β with a multiplier $1 - \varphi$ when time $t \geq t_0$. At the initial stage of an outbreak, the Malthusian parameter becomes $\lambda_\varphi = (1 - \varphi)\beta - \mu$. From a mathematical point of view, we can adjust the parameters φ, η to allow $\lambda_\varphi = \lambda_\eta$. Therefore, the above analysis can cover this scenario.

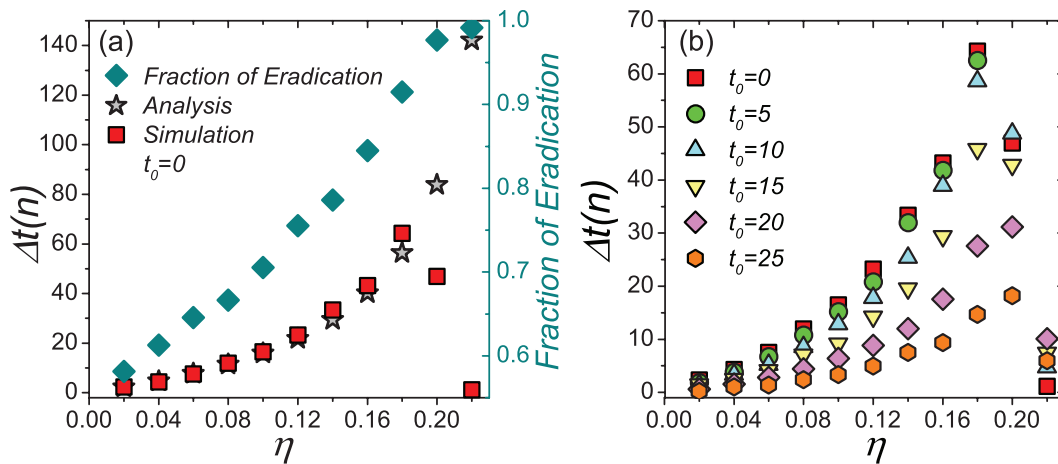


FIG. 3: (*Color online*) The effects of patient isolation in delaying disease invasion. (a) The relation between the delay of FAT, $\Delta t(\eta)$, and the isolation intensity η with $t_0 = 0$. The dark cyan diamonds show the fraction of eradication. (b) The simulation results with $t_0 = 0, 10, 15, 20,$ and 25 .

IV. SUMMARY

In sum, the intra-population interventions, e.g., patient isolation, perform better than the inter-population strategies such as travel restriction if the response time is small. Therefore, the intra-population strategies are more beneficial in delaying the spatial spread of pandemic influenza if they are implemented very promptly. However, the intra-population measures are sensitive to the increase of response time, which might be inevitable due to miscellaneous socioeconomic reasons in reality and

largely discounts the efficiency.

V. ACKNOWLEDGMENTS

This study is supported by National Key Basic Research and Development Program (No.2010CB731403), the NCET program (No.NCET-09-0317), and the National Natural Science Foundation(No. 61273223) of China.

-
- [1] R.M. Anderson, R.M. May, *Infectious Diseases of Humans: Dynamics and Control* (Oxford University Press, Oxford, U.K., 1991).
- [2] S. Boccaletti, et al., *Phys. Rep.* **424**, 175(2006).
- [3] A. Barrat, et al. *Dynamical Processes on Complex Networks*(Cambridge University Press, Cambridge, U.K., 2008).
- [4] S.N. Dorogovtsev, et al., *Rev. Mod. Phys.* **80**, 1275(2008).
- [5] A. Vespignani, *Nat. Phys.* **8**, 32(2012).
- [6] R. Pastor-Satorras and A. Vespignani, *Phys. Rev. Lett.* **86**, 3200(2001); Y. Moreno, et al., *Eur. Phys. J B* **26**, 521(2002); Boguñá M., et al., *Phys. Rev. Lett.* **90**, 028701(2003); Xia C.Y., et al., *Int. J Mod. Phys. B* **23**, 2303(2009); B. Guerra, J. Gómez-Gardeñes, *Phys. Rev. E* **82**, 035101(2010); C. Castellano and R. Pastor-Satorras, et al., *Phys. Rev. Lett.* **105**, 218701(2010).
- [7] L.A. Rvachev, and I.M. Longini, Jr., *Math. Biosci.* **75**, 3(1985); C. Viboud, et al., *Science* **312**, 447(2006); V. Colizza, et al., *Nat. Phys.* **3**, 276(2007); D. Balcan, et al., *Proc. Natl. Acad. Sci. U.S.A.* **106**, 21484(2009); Wang L., et al., *PLoS ONE* **6**, e21197(2011). H.H.K Lentz, et al., *Phys. Rev. E* **85**, 066111(2012). C. Poletto, et al., *Sci. Rep.* **2**, 476(2012).
- [8] L. Cao, et al., *Phys. Rev. E* **84**, 041936(2011)
- [9] World Health Organization, *Pandemic Influenza Preparedness and Response* (WHO, Geneva, 2009); United States Department of Health and Human Services, *HHS Pandemic Influenza Plan* (HSS, Washington, D.C., 2005).
- [10] Y. Yang, et al., *Science* **326**, 729(2009); J. Gómez-Gardeñes, et al., *Proc. Natl. Acad. Sci. U.S.A.* **105**, 1399(2008); P. Holme, *Europhys. Lett.* **68**, 908(2004); M.E. Halloran, et al., *Proc. Natl. Acad. Sci. U.S.A.* **105**, 4639(2008); Y. Chen, et al., *Phys. Rev. Lett.* **101**, 058701(2008); L. Hufnagel, et al., *Proc. Natl. Acad. Sci. U.S.A.* **101**, 15124(2004); V. Colizza, et al., *PLoS Med.* **4**, e13(2007);
- [11] I.M. Longini Jr., et al., *Science* **309**, 1083(2005).
- [12] B.S. Cooper, et al., *PLoS Med.* **3**, e212(2006).
- [13] T.D. Hollingsworth, et al., *Nat. Med.* **12**, 497(2006).
- [14] J.M. Epstein, et al., *PLoS ONE* **2**, e401(2007).
- [15] P. Bajardi, et al., *PLoS ONE* **6**, e16591(2011).
- [16] G.S. Tomba, J. Wallinga, *Math. Biosci.* **214**, 70(2008).
- [17] P. Caley, N.G. Becker, D.J. Philp, *PLoS ONE* **2**: e143(2007).
- [18] A. Gautreau, et al., *J. Stat. Mech.* L09001(2007).
- [19] A. Gautreau, et al., *J. Theor. Biol.* **251**, 509(2008).
- [20] A. Gautreau, et al., *Natl. Acad. Sci. U.S.A.* **106**, 8847(2009).

- [21] J.L. Iribarren, E. Moro, Phys. Rev. Lett. **103**, 038702(2009). [22] O. Diekmann, et al., J. R. Soc. Interface **7**, 873(2010).